

Geophysical Research Letters*



RESEARCH LETTER

10.1029/2025GL117631

Key Points:

- Soil moisture (SM) effects on surface water availability (P-E) vary significantly between nearshore and inland drylands
- In nearshore drylands, aridifying SM promotes the increase in Δ(P-E) through an increase in moisture convergence (MC) in a warmer future
- In inland drylands, humidifying SM intensifies the decrease in Δ(P-E) through a decrease in MC with global warming

Supporting Information:

Supporting Information may be found in the online version of this article.

Correspondence to:

S. Wang, wangss@lzu.edu.cn

Citation:

Hu, Y., Wang, S., Guan, X., & Huang, J. (2025). Distinct effects of soil moisture on surface water availability in nearshore and inland drylands. *Geophysical Research Letters*, 52, e2025GL117631. https://doi.org/10.1029/2025GL117631

Received 23 JUN 2025 Accepted 4 OCT 2025

Author Contributions:

Shanshan Wang
Data curation: Yuanyuan Hu,
Shanshan Wang
Formal analysis: Yuanyuan Hu,
Shanshan Wang
Methodology: Yuanyuan Hu,
Shanshan Wang
Supervision: Shanshan Wang,
XiaoDan Guan, Jianping Huang
Writing – original draft: Yuanyuan Hu,
Shanshan Wang
Writing – review & editing:

Yuanyuan Hu, Shanshan Wang

Conceptualization: Yuanvuan Hu.

© 2025. The Author(s). This is an open access article under the terms of the Creative Commons Attribution License, which permits use, distribution and reproduction in any medium, provided the original work is properly cited.

Distinct Effects of Soil Moisture on Surface Water Availability in Nearshore and Inland Drylands

Yuanyuan Hu¹, Shanshan Wang^{1,2}, XiaoDan Guan^{1,2}, and Jianping Huang^{1,2}

¹Key Laboratory for Semi-Arid Climate Change of the Ministry of Education, College of Atmospheric Sciences, Lanzhou University, Lanzhou, China, ²Collaborative Innovation Center for Western Ecological Safety, Lanzhou, China

Abstract Soil moisture (SM) substantially influences the change of surface water availability (precipitation minus evapotranspiration, P-E) in water-limited drylands by altering evapotranspiration and atmospheric water vapor inflow. While the overall significance of SM-P-E feedbacks is recognized, the spatial variability and consistency across different dryland types remain unclear. Here, we investigate these feedbacks across nearshore and inland drylands, revealing substantial heterogeneity in their responses. Using land-atmosphere coupling experiments and atmospheric moisture budget analysis, we demonstrate contrasting mechanisms: in nearshore drylands, reductions in SM trigger increased moisture convergence, mitigating precipitation decline and even elevating P-E; conversely, in inland drylands, enhancements in SM further suppress precipitation by diminishing moisture inflow, leading to a decline in P-E. These findings uncover region-specific SM-water cycle feedbacks, providing new insights into drylands water dynamics and implications for water resources management under changing climate conditions.

Plain Language Summary Globally, soil moisture (SM) is a key factor influencing surface water availability (precipitation minus evapotranspiration, P-E), and its impact is even more pronounced in drylands. Previous research has demonstrated reductions of SM facilitate moisture transport into drylands, thereby elevating local precipitation and P-E. While SM's impact on P-E is established, it's unclear if this effect is the same across all drylands, especially comparing nearshore and inland drylands. Water vapor transport and convergence may be limited around inland drylands due to scarcity of nearby water sources. The potential spatial heterogeneity of SM-P-E feedbacks within nearshore and inland drylands remains poorly understood. Therefore, this paper focuses on distinct effects of SM on P-E in nearshore (within 500 km of the coastline) and inland drylands (beyond 1,000 km from the coastline). Utilizing land-atmosphere coupling experiments and atmospheric moisture budget diagnosis, we discover SM anomaly effect induces different variations in P-E in nearshore and inland drylands. Under global warming, for nearshore drylands, drying SM promotes increased P-E through enhanced moisture convergence (MC), whereas in inland drylands, wetting SM exacerbates decreased P-E by reducing MC. This study contributes to the understanding of land-atmosphere interactions and coupling in different dryland regions, thereby informing more effective water resource management efforts.

1. Introduction

Among important land surface processes, soil moisture (SM) is a pivotal factor critically regulating the global water and energy cycles. It exerts profound control over precipitation, evapotranspiration, and consequently, surface water availability—quantified as precipitation minus evapotranspiration (P-E) (Rockström et al., 2009; Seddon et al., 2016; Zhou et al., 2022). By altering latent and sensible heat fluxes, SM can modulate surface energy distribution, thereby affecting atmospheric water vapor cycle and amplifying or mitigating climate extremes, such as drought and severe rainfall, which subsequently alter P-E patterns (Berg et al., 2016; Chen et al., 2025; Meng et al., 2014; Qiang et al., 2017; Seo & Ha, 2022; Y. Wang & Yuan, 2022; Zeng et al., 2019). Notably, SM deficits can inhibit precipitation while increasing evapotranspiration, accelerating flash drought onset, especially in humid, vegetated regions (Ma & Yuan, 2025; Y. Wang & Yuan, 2022; Yuan et al., 2023). Furthermore, in periods of droughts, SM depletion not only diminishes the intensity of water cycle but also sustains atmospheric circulation anomalies, promoting drought self-propagation (Fischer et al., 2007; Koster et al., 2014, 2016; Schumacher et al., 2022; Wu & Kinter, 2009). For example, positive SM-precipitation feedback linked to low SM has been shown to increase drought frequency in the northeastern United States (Alessi et al., 2022). Conversely, variations in SM not only lead to drought, but also exert an impact on

HU ET AL. 1 of 10

humidification process. Soil desiccation contributes to precipitation by causing an increase in evapotranspiration in the humid regions and MC in the arid regions (Qing et al., 2023).

Notably, the influence of SM on P-E exhibits pronounced regional heterogeneity, varying significantly across climate zones. This heterogeneity is particularly significant in drylands, where recent analyses reveal complex feedbacks. Beyond limiting local evapotranspiration (Denissen et al., 2020; Qiao et al., 2023; Yan et al., 2024; Yang et al., 2018), the reduction in SM can enhance moisture transport into the drylands by modulating atmospheric circulation and vertical uplift. This imported moisture can facilitate precipitation, partially offsetting declines in drylands P-E (Qing et al., 2023; Zhou et al., 2021). This inspires a fundamental question of whether such SM anomaly effects on P-E perform consistent across all drylands, specifically between nearshore and inland drylands.

We hypothesize significant divergence in SM's influence on atmospheric water vapor transport and P-E between nearshore and inland drylands. Reduced SM in nearshore drylands may efficiently drive convergent circulations that draw in maritime moisture. In contrast, similar circulations triggered by SM reduction in inland drylands are likely constrained by the scarcity of nearby water vapor sources (Cao et al., 2025; Cheng et al., 2021). This potential spatial heterogeneity in SM-P-E feedbacks within drylands—distinguishing nearshore from inland dynamics—remains inadequately understood and constitutes a critical knowledge gap.

Consequently, this study addresses this gap by systematically investigating the differential effects of SM on P-E in nearshore versus inland drylands. Based on model simulations from CMIP6 and LFMIP-pdLC, our results suggest spatial heterogeneity in SM-P-E feedbacks in drylands based on future simulations of CMIP6 and LFMIP-pdLC. Our findings provide a novel and crucial contribution to understanding land-atmosphere interactions in diverse drylands environments, offering valuable insights for regional water resource management and climate change adaptation.

2. Data and Methods

2.1. Data

In the research, we select monthly data from six CMIP6 models for precipitation ("pr"), moisture in upper portion of soil column ("mrsos," 0–10 cm), latent heat flux ("hfls"), and air temperature ("tas"), covering both the historical period (1980–2014) and the far future period (2066–2100, SSP585 scenario). Besides, for each model, we choose one ensemble member (see Table S1 in Supporting Information S1 for details). Critically, only the six CMIP6 models (CESM2, CMCC-ESM2, CNRM-CM6-1, EC-Earth3, IPSL-CM6A-LR, and MPI-ESM12-LR) both participate in LFMIP-pdLC experiment and contain the required variables. Furthermore, these models have empirically demonstrated superior performance on other variables, such as SM and P-E (Qiao et al., 2023; Zhou et al., 2022).

As certain models lack direct data for evapotranspiration, we opt to derive evapotranspiration through air temperature (T) and latent heat flux (LE). Accordingly, evapotranspiration can be decomposed into the following components (Allen et al., 1998)

$$E = \frac{LE}{2.501 - (2.361 * 10^{-3})T}$$
 (1)

where the unit of T is °C.

2.2. Definition of the Nearshore and Inland Drylands

To study the variation in P-E due to heterogeneity in SM, we categorize drylands into the nearshore and inland drylands. However, there is no clear criterion for the division of nearshore and inland drylands. Standards for the classification of nearshore drylands versus inland drylands vary according to disciplinary background and research objectives. Under the United Nations Convention on the Law of the Sea, 200 nautical miles (approximately 370 km) is defined as the exclusive economic zone. However, from the meteorological perspective, as the monsoon continues to advance, water vapor from the ocean can be transported inland (Cai et al., 2024). In particular, the East Asian monsoon moisture transport can reach northwestern China (more than 1,000 km from

HU ET AL. 2 of 10

the coastline) (Ding & Chan, 2005), while the Australian monsoon can bring Australian monsoon rainfall and provide most of the freshwater for northern Australia (less than 500 km from the coastline) (Heidemann et al., 2023). Therefore, in our study, drylands less than 500 km from the coastline are chosen to be defined as nearshore drylands, and drylands more than 1,000 km from the coastline are defined as inland drylands.

2.3. Definition of Aridity Index

The aridity index (AI) (Li et al., 2015) can be calculated from precipitation and potential evapotranspiration (PET).

$$AI = \frac{P}{PET}$$
 (2)

Drylands are defined as the regions with the AI less than or equal to 0.65 (Li et al., 2015; Middleton & Thomas, 1997; Mortimore, 2009). In order to better analyze the distribution of drylands, we download the AI from the third edition of the global desiccation index and potential evapotranspiration database which is provided by Plant Data Center of Chinese Academy of Sciences (Trabucco & Zomer, 2008, 2019; Zomer et al., 2022). Within this data set, the PET is computed utilizing the FAO-56 Penman-Monteith equation, a well-established method that effectively integrates both energy balance and the aerodynamic mass transfer method for its calculations (Zomer et al., 2022).

2.4. Moisture Budget Decomposition

Based on moisture budget decomposition (Zhou et al., 2022), the primary moisture sources for precipitation (P) are evapotranspiration (E) and MC. Calculated from the top of the atmosphere (p = 0) to the ground ($p = p_s$) at air pressure (p), MC is characterized as the negative divergence of the vertical integral moisture flux.

$$P = E + MC \tag{3}$$

$$MC = -\frac{1}{\rho_w g} \nabla \cdot \int_0^{\rho_s} (uq) \, dp \tag{4}$$

In the above equations, ρ_w is the density of water, g represents the acceleration of gravity, ∇ is the operator for horizontal divergence, u is the horizontal vector wind, and g is the specific humidity.

Because we use monthly data sets in this research and pay attention to climatological change, overbars represent monthly averages.

$$MC \approx -\frac{1}{\rho_w g} \nabla \cdot \int_0^{p_s} (\overline{u} \cdot \overline{q}) dp \tag{5}$$

Besides, we use the subscript 0 to represent the historical period. The MC in the historical period (MC_0) can be decomposed as

$$MC_0 \approx -\frac{1}{\rho_{ss}g} \nabla \cdot \int_0^{p_s} \left(\overline{u_0} \cdot \overline{q_0} \right) dp$$
 (6)

Subtracting the above two equations, we can calculate the change from the historical to future periods in MC (ΔMC) as

$$\Delta MC \approx -\frac{1}{\rho_w g} \nabla \cdot \int_0^{p_s} \left(\overline{u_0} \cdot \Delta \overline{q} + \overline{q_0} \cdot \Delta \overline{u} + \Delta \overline{u} \cdot \Delta \overline{q} \right) dp \tag{7}$$

Next, according to the mass continuity equation (Bony et al., 2013),

HU ET AL. 3 of 10

$$-\frac{1}{\rho_{w}g}\nabla \cdot \int_{0}^{p_{s}} \left(\overline{q_{0}} \cdot \Delta \overline{u}\right) dp = -\frac{1}{\rho_{w}g} \int_{0}^{p_{s}} \left(\Delta \overline{\omega} \cdot \frac{\partial q}{\partial p}\right) dp \tag{8}$$

where ω is the pressure vertical velocity, so we can denote Δ MC as

$$\Delta MC \approx -\frac{1}{\rho_w g} \nabla \cdot \int_0^{p_s} (\overline{u_0} \cdot \Delta \overline{q} + \Delta \overline{u} \cdot \Delta \overline{q}) dp - \frac{1}{\rho_w g} \int_0^{p_s} (\Delta \overline{\omega} \cdot \frac{\partial q}{\partial p}) dp$$
 (9)

From the above equation, we can find ΔMC can be influenced by three terms, which are a thermodynamic term $(-\frac{1}{\rho_w g} \nabla \cdot \int_0^{p_s} (\overline{u_0} \cdot \Delta \overline{q}) \, dp)$, a dynamic term $(-\frac{1}{\rho_w g} \int_0^{p_s} (\Delta \overline{w} \cdot \frac{\partial q}{\partial p}) \, dp)$, and a nonlinear term $(-\frac{1}{\rho_w g} \nabla \cdot \int_0^{p_s} (\Delta \overline{u} \cdot \Delta \overline{q}) \, dp)$.

2.5. Soil Moisture-Atmosphere Feedback Experiments

In this paper, we utilize the output generated by the Land Feedback Model Intercomparison Project with prescribed Land Conditions (LFMIP-pdLC, Hurk et al., 2016), where these prescribed land conditions are derived from the average annual cycle of historical global climate model simulations from 1980 to 2014. With fully coupled models provided by CMIP6, the SM anomaly effect on P-E can be quantified by analyzing the difference between CMIP6 and LFMIP-pdLC (non-SM anomaly effect). Consequently, the MC changes discussed in this paper are primarily a consequence of local circulation anomalies, which are linked to SM variations.

3. Results

3.1. Distinct SM Anomaly Effects on P-E in Nearshore and Inland Drylands

Our analysis begins by examining projected SM changes between the far future (2066–2100) and historical period (1980–2014) across drylands, specifically contracting nearshore and inland drylands. Notably, the significant variation of SM in drylands exhibits spatial heterogeneity, primarily characterized by decreases in nearshore drylands (72.7% of grid cells with negative SM anomalies) and increases in inland drylands (75% of grid cells show positive SM anomalies) (Figures 1a and 1b), which are corroborated by other studies (Zhao & Dai, 2022; Zhou et al., 2021).

Critically, the effect of these SM changes on precipitation (ΔP), evapotranspiration (ΔE), and consequently surface water availability (Δ (P-E)) exhibits fundamentally different patterns between the two dryland types. For nearshore drylands (Figures 1c, 1e, and 1g), a significant decline in SM is associated with considerable decreases in both ΔP and ΔE . ΔE , however, exhibited a substantially steeper decline. Consequently, this leads to a net enhancement in Δ (P-E) across key regions like the southwestern United States, the Mediterranean coast, southern South America, southern Africa and Australia. Absent the influence of SM anomaly effect, the local aridification driven by the decrease in $\Delta(P-E)$ would likely proceed at an accelerated rate (Tripathi et al., 2024, Figure S2 in Supporting Information S1). In inland drylands (Figures 1d, 1f, and 1h), increasing SM anomaly effect produces more complex response. In the Sahel, increased SM causes a decrease in ΔP alongside a significant increase of ΔE , further exacerbating the decrease in $\Delta (P-E)$. It may result from SM-enhanced evapotranspiration inducing surface cooling, which inhibits convective activity and further reduces local precipitation (F. Wang et al., 2023). In Middle East Asia, a substantial increase in SM leads to increases in ΔP and ΔE , contributing to regional moistening trend (Liang et al., 2025; Y. Wang et al., 2017; Zhang et al., 2023). However, the larger increase in ΔE results in a net decrease in $\Delta(P-E)$. Consequently, SM's changes promote increased $\Delta(P-E)$ in most nearshore drylands while exacerbating decreased $\Delta(P-E)$ in inland drylands. This contrast is fundamentally linked to the heterogeneous future SM trajectory (decrease in nearshore drylands, increase in inland drylands) and its divergent impacts on the regional water cycle (Sun et al., 2025). In the warmer future, the changes of precipitation, evapotranspiration, and P-E are dominated by non-SM anomaly effect (Figures S1 and S2 in Supporting Information S1), which causes a decrease in $\Delta(P-E)$ in nearshore drylands and an increase in inland drylands. However, by mitigating the detrimental effects of the non-SM anomaly effect, the SM anomaly effect plays a crucial role in stabilizing the water cycle in water-limited drylands.

HU ET AL. 4 of 10

19448007, 2025, 20, Downloaded from https://agupubs.onlinelibrary.wiey.com/doi/10.1029/2025GL117631 by Lauzhou University, Wiley Online Library on [05/11/2025]. See the Terms and Conditions (https://onlinelibrary.wiley.com/emw

on Wiley Online Library for rules of

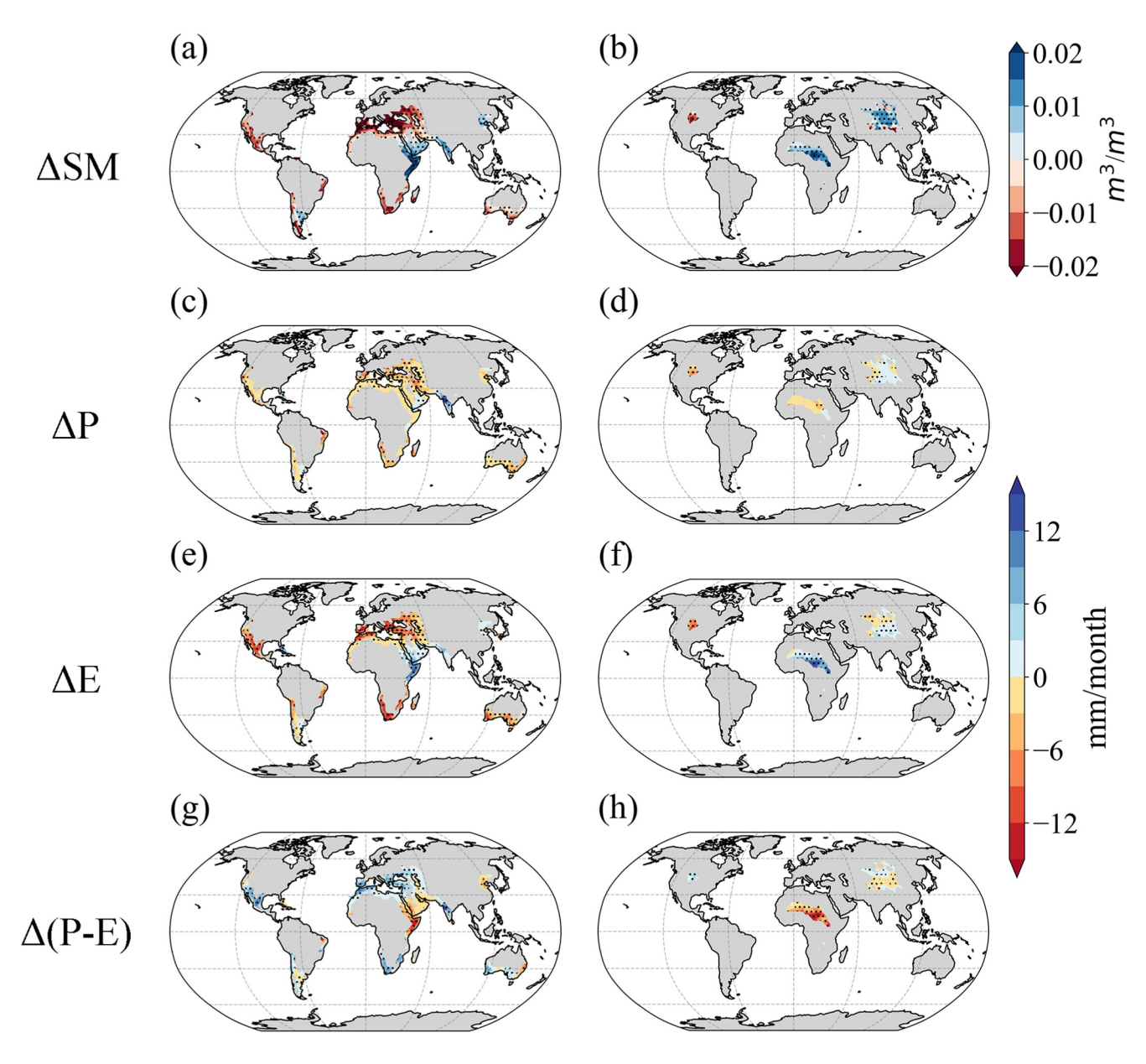


Figure 1. Soil moisture (SM) anomaly effects on precipitation, evapotranspiration, and surface water availability in the nearshore and inland drylands. (a, b) Multi-model mean changes of SM (Δ SM) in the nearshore and inland drylands between 1980–2014 (historical simulation) and 2066–2100 (SSP585 simulation) in the six CMIP6 models which participate in the LFMIP-pdLC experiment. (c–h) SM anomaly effects on the changes of precipitation (Δ P), evapotranspiration (Δ E), and surface water availability (Δ (P-E)) in drylands assessed as CMIP6 minus LFMIP-pdLC results. Stippling denotes regions where the sign of Δ P, Δ E, and Δ (P-E) is consistent with the sign of multi-model means (as shown in the figure) for at least 4 of the 6 models.

3.2. Divergent Mechanisms of SM Anomaly Effect in Nearshore and Inland Drylands

To further explore the mechanism driving these above contrasting impacts, we conduct the atmospheric moisture budget diagnosis of the SM anomaly effect between nearshore and inland regions of the drylands. In nearshore drylands, SM's decrease reduces evapotranspiration (Figure 2a). Crucially, it also triggers enhanced MC, primarily driven by the thermodynamic and dynamic terms. This imported moisture partially offsets the reduction in local precipitation caused by lower evapotranspiration. The net result is a weaker precipitation response compared to the evapotranspiration reduction, which is consistent with Zhou et al. (2021), leading to an increase in local P-E.

HU ET AL. 5 of 10

19448007, 2025, 20, Downloaded from https://agupubs.onlinelibrary.wiley.com/doi/10.1029/2025GL117631 by Lanzhou University, Wiley Online Library on [05/11/2025]. See the Terms

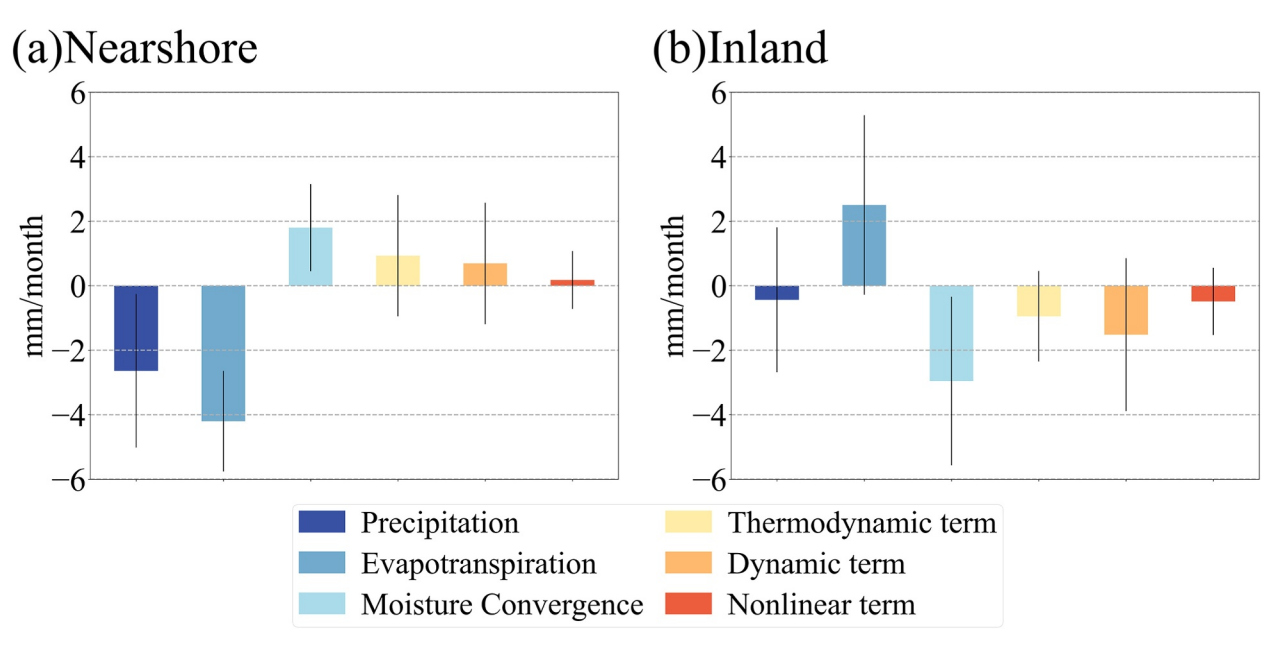


Figure 2. Mechanisms of the Soil moisture (SM) anomaly effects on surface water availability in the nearshore and inland drylands. (a) SM anomaly effects on changes in precipitation, evapotranspiration, moisture convergence (MC), and the thermodynamic, dynamic, and nonlinear terms of MC in the nearshore drylands between 1980–2014 and 2066–2100. (b) The same as (a) but for the inland drylands. The error bar shows the standard deviation of each variable in the 6 models.

Over inland drylands, the wetting SM drives increased evapotranspiration, which is favorable for local precipitation generation (Figure 2b). However, this positive effect is overwhelmed by a concurrent reduction in MC (or increase in moisture divergence), induced by the moistening SM through both thermodynamic and dynamic processes. This decreased convergence significantly inhibits precipitation, outweighing the contribution from increased evapotranspiration. Consequently, the net precipitation response to SM increase is negative. Further, atmospheric moisture budget diagnosis confirms that the reduction in precipitation is exacerbated by the cumulative effect of decreased MC, which also strongly intensifies the diminishment in P-E.

These mechanistic findings are fully consistent with the spatial distribution of SM anomaly effects described in Section 3.1 (Figure 1). We identify that in nearshore (inland) drylands, drier (wetter) SM conditions under future warming enhance (reduce) Δ (P-E) through increased (decreased) MC, which may further contribute local wetting (drying) of SM. Consequently, SM-driven P-E changes can establish a negative feedback loop for subsequent SM evolution. Understanding this feedback mechanism is crucial for improving future SM projections in drylands and contributing to the conservation of local ecosystems (Deng et al., 2020; Kannenberg et al., 2024; Lian et al., 2021; Wankmüller et al., 2024).

3.3. Regional Manifestations of SM Anomaly Effect in Typical Drylands

Based on the classification of the nearshore and inland regions of the drylands, we examine seven typical dryland regions: five dryland areas in the nearshore drylands (Figure 3a), including the southwestern United States, southern South America, southern Africa, the Mediterranean coast, and Australia, and two dryland areas in the inland drylands (Figure 3b), namely, the Sahel and the Middle East Asia, as shown in Figure 3. In the five dryland areas of nearshore drylands (Figures 3c–3g), we consistently observe that decreasing SM reduces evapotranspiration while simultaneously stimulating the convergence of moisture from the ocean. This stimulation is driven by the combined influence of the thermodynamic and dynamic terms, ultimately moderating the reduction in precipitation caused by lower evapotranspiration. Consequently, in nearshore drylands, the effect of SM contributes to an overall increase in P-E, thereby mitigating local droughts. In addition, for inland drylands (Figures 3h and 3i), increased SM promotes an increase in evapotranspiration, which would provide more favorable water vapor conditions for precipitation generation. However, the SM anomaly effect also drives a more substantial reduction in MC. This net reduction in MC, outweighing the benefits of the increased evapotranspiration, leads to less precipitation and further exacerbating the decrease in P-E.

HU ET AL. 6 of 10

19448007, 2025, 20, Downloaded from https://agupubs.onlinelibrary.wiley.com/doi/10.1029/2025GL117631 by Lanzhou University, Wiley Online Library on [05/11/2025]. See the Terms and Conditions (https://agupubs.onlinelibrary.wiley.com/doi/10.1029/2025GL117631 by Lanzhou University, Wiley Online Library on [05/11/2025]. See the Terms and Conditions (https://agupubs.onlinelibrary.wiley.com/doi/10.1029/2025GL117631 by Lanzhou University, Wiley Online Library on [05/11/2025]. See the Terms and Conditions (https://agupubs.onlinelibrary.wiley.com/doi/10.1029/2025GL117631 by Lanzhou University, Wiley Online Library on [05/11/2025]. See the Terms and Conditions (https://agupubs.onlinelibrary.wiley.com/doi/10.1029/2025GL117631 by Lanzhou University, Wiley Online Library on [05/11/2025]. See the Terms and Conditions (https://agupubs.onlinelibrary.wiley.com/doi/10.1029/2025GL117631 by Lanzhou University, Wiley Online Library.wiley.com/doi/10.1029/2025GL117631 by Lanzhou University.wiley.com/doi/10.1029/2025GL117631 by Lanzhou Universit

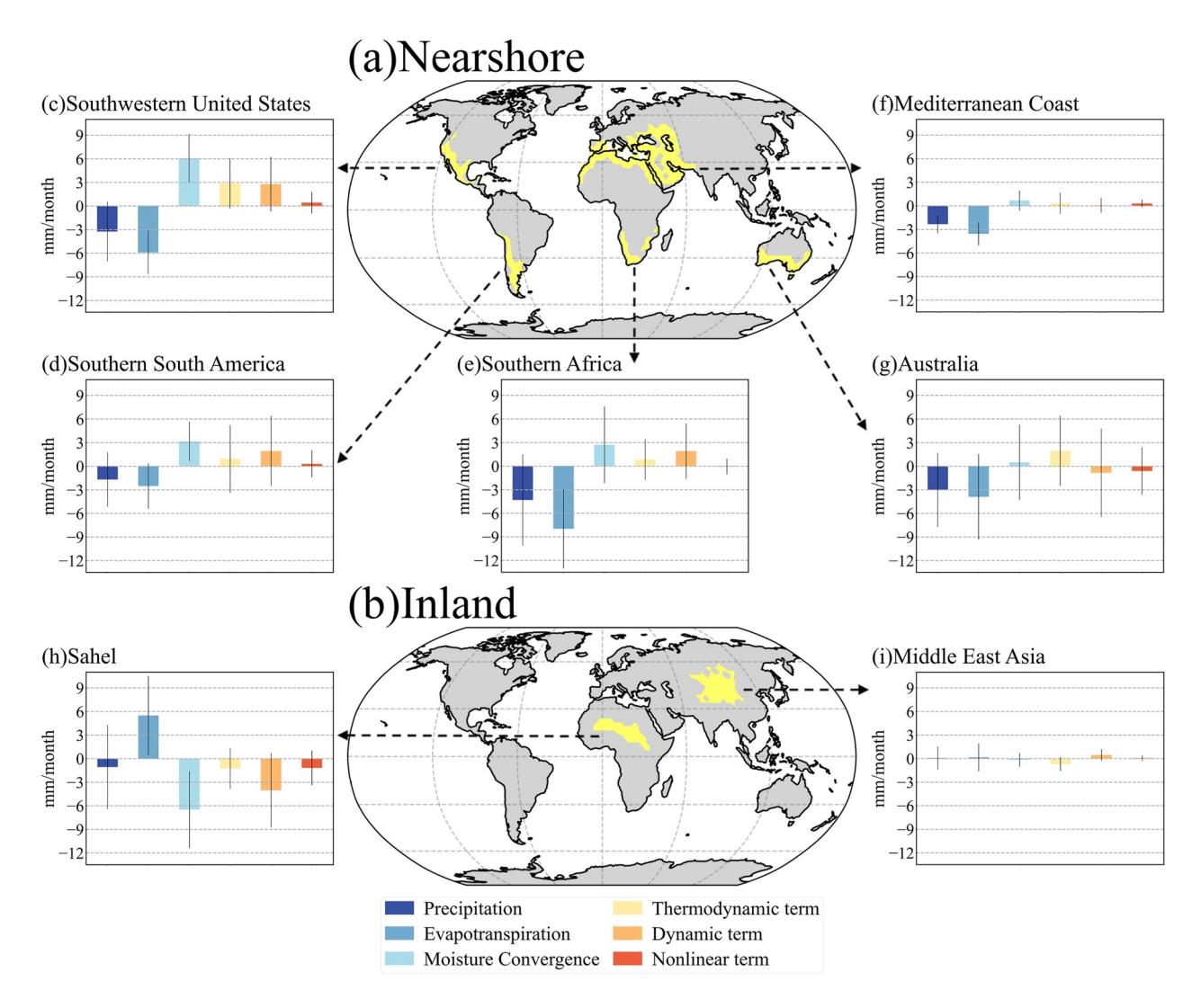


Figure 3. Mechanisms of the Soil moisture (SM) anomaly effects on surface water availability in different regions of the nearshore and inland drylands. (a, b) The spatial distribution of typical regions in the nearshore and inland drylands. (c) SM anomaly effects on the changes in precipitation, evapotranspiration, moisture convergence (MC), and the thermodynamic, dynamic, and nonlinear terms of MC in southwestern United States between 1980–2014 and 2066–2100. (d–i) The same as (c) but for southern South America, southern Africa, the Mediterranean coast, Australia, the Sahel, and the Middle East Asia, respectively.

In summary, atmospheric moisture budget diagnosis reveals divergent mechanisms of SM anomaly effect in nearshore and inland drylands under a warmer future: drier SM promotes increased P-E in nearshore drylands, whereas wetter SM inhibits P-E in inland drylands. These contrasting pathways are mediated by changes in MC.

4. Conclusion and Discussion

Previous studies have found that decreasing SM drives MC in drylands (Qing et al., 2023; Zhou et al., 2021). However, due to the known difficulties in transporting moisture to inland regions of drylands, it remains uncertain whether the same mechanism applies. To fully understand this gap, our study analyzes the underlying heterogeneity of the impacts of SM on P-E in both nearshore and inland of drylands. Therefore, in this research, we examine that the influence of SM on P-E in nearshore and inland of drylands through model comparison between CMIP6 and LFMIP-pdLC experiment, and the atmospheric moisture budget diagnosis.

Utilizing six models which participate in the LFMIP-pdLC experiment between 1980–2014 (historical simulation) and 2066–2100 (SSP585 simulation), comparing the SM anomaly effect obtained from the CMIP6 and LFMIP-pdLC experiments (Figure 1), and then analyzing the atmospheric moisture budget diagnosis of the SM anomaly effect (Figures 2 and 3), we can find distinct effects of SM on P-E in nearshore and inland drylands and

HU ET AL. 7 of 10

19448007, 2025, 20, Downloaded from https://agupubs.onlinelibrary.wiley.com/doi/10.1029/2025GL117631 by Lanzhou University, Wiley Online Library on [05/11/2025]. See the Terms and Co

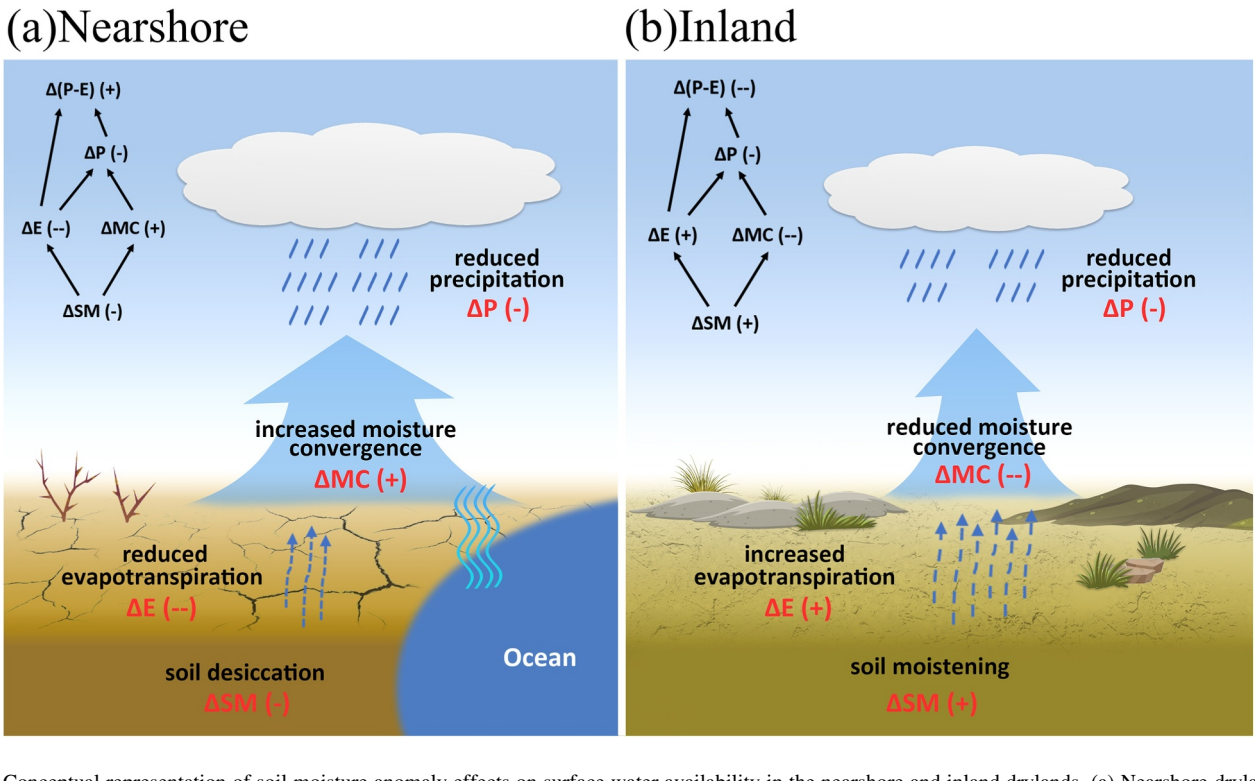


Figure 4. Conceptual representation of soil moisture anomaly effects on surface water availability in the nearshore and inland drylands. (a) Nearshore drylands: Soil desiccation induces a decrease in evapotranspiration, while simultaneously promoting the convergence of moisture from the ocean, thereby elevating atmospheric moisture and partially mitigating the decline of precipitation. (b) Inland drylands: Although soil moistening contributes to an increase in evapotranspiration, the decreased convergence of moisture leads to a more pronounced decline in precipitation.

further draw the conceptual diagram (Figure 4). For nearshore drylands (Figure 4a), a reduction in SM results in a decrease in evapotranspiration but also triggers a greater convergence of moisture from the ocean to these areas. The elevated MC partially offsets the decline in precipitation, leading to a more pronounced decrease in evapotranspiration relative to precipitation and consequently increasing the P-E, which contributes to local drought mitigation (Delgado-Baquerizo et al., 2013; Tripathi et al., 2024; Yao et al., 2023). And conversely, in inland drylands (Figure 4b), an increase in SM causes evapotranspiration to enhance, while MC decreases. Because the substantial reduction in MC completely offsets the precipitation resulting from the increase in evapotranspiration, there is a net decrease in precipitation. Accordingly, the reduction in the P-E is amplified.

Nearshore drylands, due to their proximity to the ocean, benefit from a continuous supply of external water vapor (Abbott et al., 2019; Oki et al., 2004; Palmer, 2014). This dominance of the external water cycle is conducive to an increase in MC. However, inland drylands are more dependent on local water vapor, resulting in a dominance of the internal water cycle and restricting potential increase of MC. Despite our specific choice of 500 and 1,000 km to define the nearshore and inland drylands, this finding remains robust. We observe highly consistent conclusions when trying alternative demarcation criteria, such as 200 nautical miles and 800 km, reinforcing the results presented in this paper (Figure S3 in Supporting Information S1). Due to nonlinear interactions and model uncertainty, we have not considered local components and have not separated the effects of evapotranspiration on precipitation facilitation or suppression, but this limitation does not affect the main conclusions. We will try to address related issues in the future. Additionally, addressing the challenges of water resource management and climate change adaptation in the face of intensifying drought requires both accurate models capable of generating reliable P-E predictions (IPCC, 2023; Piedrahita et al., 2024; Yin et al., 2023) and a deeper understanding of the complexity of P-E dynamics in inland drylands. While idealized hydrological models may suggest a tendency toward a stable P-E value, observations reveal a far more intricate reality. This complexity is actively studied by other researchers (Konapala et al., 2020; Zhou et al., 2021, 2022), whose work provides vital scientific insights that underpin effective water resource management, ecological conservation, and climate change adaptation.

HU ET AL. 8 of 10

Conflict of Interest

The authors declare no conflicts of interest relevant to this study.

Data Availability Statement

There is online access to all the data used in this study. The CMIP6 (including LFMIP-pdLC) model simulations are obtained from https://esgf-node.ipsl.upmc.fr/projects/cmip6-ipsl/. Besides, the third edition of the global desiccation index and potential evapotranspiration database provided by Plant Data Center of Chinese Academy of Sciences is from https://www.plantplus.cn/doi/doi.org/10.6084.

Acknowledgments

This study is jointly supported by the National Science Foundation of China (42522503, 42475023, and 423B2501).

References

- Abbott, B. W., Bishop, K., Zarnetske, J. P., Minaudo, C., Chapin, F. S., Krause, S., et al. (2019). Human domination of the global water cycle absent from depictions and perceptions. *Nature Geoscience*, 12(7), 533–540. https://doi.org/10.1038/s41561-019-0374-y
- Alessi, M. J., Herrera, D. A., Evans, C. P., Degaetano, A., & Ault, T. R. (2022). Soil moisture conditions determine land-atmosphere coupling and drought risk in the northeastern United States. *Journal of Geophysical Research: Atmospheres*, 127(6), e2021JD034740. https://doi.org/10.1029/2021JD034740
- Allen, R. G., Pereira, L. S., Raes, D., & Smith, M. (1998). Crop evapotranspiration: Guidelines for computing crop water requirements. FAO Irrigation and Drainage Paper 56.
- Berg, A., Findell, K., Lintner, B., Giannini, A., Seneviratne, S. I., Van Den Hurk, B., et al. (2016). Land-atmosphere feedbacks amplify aridity increase over land under global warming. *Nature Climate Change*, 6(9), 869–874. https://doi.org/10.1038/nclimate3029
- Bony, S., Bellon, G., Klocke, D., Sherwood, S., Fermepin, S., & Denvil, S. (2013). Robust direct effect of carbon dioxide on tropical circulation and regional precipitation. *Nature Geoscience*, 6, 447–451. https://doi.org/10.1038/ngeo1799
- Cai, Q., Chen, W., Chen, S.-F., Xie, S.-P., Piao, J., Ma, T., & Lan, X. (2024). Recent pronounced warming on the Mongolian Plateau boosted by internal climate variability. *Nature Geoscience*, 17(3), 181–188. https://doi.org/10.1038/s41561-024-01377-6
- Cao, D., Cao, X., Chen, D., Du, Y., Luo, Y., Hu, Y., et al. (2025). Two types of heavy precipitation in the southeastern Tibetan Plateau. Science Bulletin, 70(5), 748–755. https://doi.org/10.1016/j.scib.2024.12.031
- Chen, C., Wang, S., Wang, Z., & Li, X. (2025). Differential impacts of sub-daily precipitation on temperature extremes across China's climatic zones. Geophysical Research Letters, 52(9), e2024GL114088. https://doi.org/10.1029/2024GL114088
- Cheng, T. F., Lu, M., & Dai, L. (2021). Moisture channels and pre-existing weather systems for East Asian rain belts. *Npj Climate and Atmospheric Science*, 4(1), 32. https://doi.org/10.1038/s41612-021-00187-6
- Delgado-Baquerizo, M., Maestre, F. T., Gallardo, A., Bowker, M. A., Wallenstein, M. D., Quero, J. L., et al. (2013). Decoupling of soil nutrient cycles as a function of aridity in global drylands. *Nature*, 502(7473), 672–676. https://doi.org/10.1038/nature12670
- Deng, Y., Wang, S., Bai, X., Luo, G., Wu, L., Cao, Y., et al. (2020). Variation trend of global soil moisture and its cause analysis. *Ecological Indicators*, 110, 105939. https://doi.org/10.1016/j.ecolind.2019.105939
- Denissen, J. M., Teuling, A. J., Reichstein, M., & Orth, R. (2020). Critical soil moisture derived from satellite observations over Europe. *Journal of Geophysical Research: Atmospheres*, 125(6), e2019JD031672. https://doi.org/10.1029/2019JD031672
- Ding, Y., & Chan, J. C. L. (2005). The East Asian summer monsoon: An overview. *Meteorology and Atmospheric Physics*, 89(1–4), 117–142. https://doi.org/10.1007/s00703-005-0125-z
- Fischer, E. M., Seneviratne, S. I., Lüthi, D., & Schr, C. (2007). Contribution of land-atmosphere coupling to recent European summer heat waves. Geophysical Research Letters, 34(6), L06707. https://doi.org/10.1029/2006GL029068
- Heidemann, H., Cowan, T., Henley, B. J., Ribbe, J., Freund, M., & Power, S. (2023). Variability and long-term change in Australian monsoon rainfall: A review. WIREs Climate Change, e823(3), e823. https://doi.org/10.1002/wcc.823
- Hurk, B. V., Kim, H., Krinner, G., Seneviratne, S. I., Derksen, C., Oki, T., et al. (2016). LS3MIP (v1.0) contribution to CMIP6: The land surface, snow and soil moisture model intercomparison project aims, setup and expected outcome. Geoscientific Model Development, 9(8), 2809–2832. https://doi.org/10.5194/gmd-9-2809-2016
- IPCC. (2023). In H. Lee & J. Romero (Eds.), Climate change 2023: Synthesis report. Contribution of working groups I, II and III to the sixth assessment report of the intergovernmental panel on climate change (core writing team). Intergovernmental Panel on Climate Change. https://doi.org/10.59327/IPCC/AR69789291691647
- Kannenberg, S. A., Anderegg, W. R. L., Barnes, M. L., Dannenberg, M. P., & Knapp, A. K. (2024). Dominant role of soil moisture in mediating carbon and water fluxes in dryland ecosystems. *Nature Geoscience*, 17(1), 20–43. https://doi.org/10.1038/s41561-023-01351-8
- Konapala, G., Mishra, A. K., Wada, Y., & Mann, M. E. (2020). Climate change will affect global water availability through compounding changes in seasonal precipitation and evaporation. *Nature Communications*, 11(1), 3044. https://doi.org/10.1038/s41467-020-16757-w
- Koster, R. D., Chang, Y., & Schubert, S. D. (2014). A mechanism for land–atmosphere feedback involving planetary wave structures. *Journal of Climate*, 27(24), 9290–9301. https://doi.org/10.1175/JCLI-D-14-00315.1
- Koster, R. D., Chang, Y., Wang, H., & Schubert, S. D. (2016). Impacts of local soil moisture anomalies on the atmospheric circulation and on remote surface meteorological fields during boreal summer: A comprehensive analysis over North America. *Journal of Climate*, 29(20), 7345–7364. https://doi.org/10.1175/JCLI-D-16-0192.1
- Li, Y., Huang, J., Ji, M., & Ran, J. (2015). Dryland expansion in northern China from 1948 to 2008. Advances in Atmospheric Sciences, 32(6), 870–876. https://doi.org/10.1007/s00376-014-4106-3
- Lian, X., Piao, S., Chen, A., Huntingford, C., Fu, B., Li, L. Z. X., et al. (2021). Multifaceted characteristics of dryland aridity changes in a warming world. *Nature Reviews Earth & Environment*, 2(4), 232–250. https://doi.org/10.1038/s43017-021-00144-0
- Liang, Q., Chen, Y., Duan, W., Wang, C., Li, Y., Zhu, J., et al. (2025). Temporal and spatial changes of extreme precipitation and its related large-scale climate mechanisms in the arid region of northwest China during 1961–2022. *Journal of Hydrology*, 658, 133182. https://doi.org/10.1016/j.jhydrol.2025.133182
- Ma, F., & Yuan, X. (2025). The propagation from atmospheric flash drought to soil flash drought and its changes in a warmer climate. *Journal of Hydrology*, 654, 132877. https://doi.org/10.1016/j.jhydrol.2025.132877

HU ET AL. 9 of 10

- Meng, X. H., Evans, J. P., & McCabe, M. F. (2014). The impact of observed vegetation changes on land–atmosphere feedbacks during drought. Journal of Hydrometeorology, 15(2), 759–776. https://doi.org/10.1175/JHM-D-13-0130.1
- Middleton, N. J., & Thomas, D. S. G. (1997). World atlas of desertification (2nd ed., p. 182). Edward Arnold.
- Mortimore, M. (2009). Dryland opportunities (p. 98). Island Press.
- Oki, T., Entekhabi, D., & Harrold, T. I. (2004). The global water cycle. In R. S. J. Sparks & C. J. Hawkesworth (Eds.), *The state of the planet: Frontiers and challenges in geophysics, IUGG* (Vol. 19, pp. 225–237). American Geophysical Union.
- Palmer, L. (2014). The next water cycle. Nature Climate Change, 4(12), 949–950. https://doi.org/10.1038/nclimate2420
- Piedrahita, V. A., Roberts, A. P., Rohling, E. J., Heslop, D., Zhao, X., Galeotti, S., et al. (2024). Dry hydroclimates in the late Palaeocene-early Eocene hothouse world. *Nature Communications*, 15(1), 7042. https://doi.org/10.1038/s41467-024-51430-6
- Qiang, Z., Hongli, Z., Liang, Z., & Ping, Y. (2017). Study on summer monsoon transition zone and its land-air interaction. Advances in Earth Science, 32, 1009–1019. https://doi.org/10.11867/j.issn.1001-8166.2017.10.1009
- Qiao, L., Zuo, Z., Zhang, R., Piao, S., Xiao, D., & Zhang, K. (2023). Soil moisture-atmosphere coupling accelerates global warming. *Nature Communications*, 14(1), 4908. https://doi.org/10.1038/s41467-023-40641-y
- Qing, Y., Wang, S., Yang, Z., & Gentine, P. (2023). Soil moisture—atmosphere feedbacks have triggered the shifts from drought to pluvial conditions since 1980. Communications Earth & Environment, 4(1), 254. https://doi.org/10.1038/s43247-023-00922-2
- Rockström, J., Falkenmark, M., Karlberg, L., Hoff, H., Rost, S., & Gerten, D. (2009). Future water availability for global food production: The potential of green water for increasing resilience to global change. *Water Resources Research*, 45, W00A12. https://doi.org/10.1029/2007WR006767
- Schumacher, D. L., Keune, J., Dirmeyer, P., & Miralles, D. G. (2022). Drought self-propagation in drylands due to land-atmosphere feedbacks. Nature Geoscience, 15(4), 262–268. https://doi.org/10.1038/s41561-022-00912-7
- Seddon, A. W., Macias-Fauria, M., Long, P. R., Benz, D., & Willis, K. J. (2016). Sensitivity of global terrestrial ecosystems to climate variability. Nature, 531(7593), 229–232. https://doi.org/10.1038/nature16986
- Seo, Y. W., & Ha, K. J. (2022). Changes in land-atmosphere coupling increase compound drought and heatwaves over northern east Asia. *Npj Climate and Atmospheric Science*, 5(1), 100. https://doi.org/10.1038/s41612-022-00325-8
- Sun, W., Zhou, S., Yu, B., Zhang, Y., Keenan, T. F., & Fu, B. (2025). Soil moisture-atmosphere interactions drive terrestrial carbon-water trade-offs. Communications Earth & Environment, 6(1), 169. https://doi.org/10.1038/s43247-025-02145-z
- Trabucco, A., & Zomer, R. (2019). Global aridity index and potential evapotranspiration (ET0) climate database v2 [Dataset]. figshare. https://doi.org/10.6084/m9.figshare.7504448.v3
- Trabucco, A., & Zomer, R. J. (2008). Global aridity index and PET database v1 (Global_AI_PET_v1) [Dataset]. CGIAR-CSI. Retrieved from https://cgiarcsi.community/data/global-aridity-and-pet-database/
- Tripathi, I. M., Mahto, S. S., Kushwaha, A. P., Kumar, R., Tiwari, A. D., Sahu, B. K., et al. (2024). Dominance of soil moisture over aridity in explaining vegetation greenness across global drylands. *Science of the Total Environment*, 917, 170482. https://doi.org/10.1016/j.scitotenv. 2024.170482
- Wang, F., Notaro, M., Yu, Y., & Mao, J. (2023). Deficient precipitation sensitivity to Sahel land surface forcings among CMIP5 models. *International Journal of Climatology*, 43(1), 99–122. https://doi.org/10.1002/joc.7737
- Wang, Y., & Yuan, X. (2022). Land-atmosphere coupling speeds up flash drought onset. Science of the Total Environment, 851, 158109. https://doi.org/10.1016/j.scitotenv.2022.158109
- Wang, Y., Zhou, B., Qin, D., Wu, J., Gao, R., & Song, L. (2017). Changes in mean and extreme temperature and precipitation over the arid region of northwestern China: Observation and projection. *Advances in Atmospheric Sciences*, 34(3), 289–305. https://doi.org/10.1007/s00376-016-6160-5
- Wankmüller, F. J. P., Delval, L., Lehmann, P., Baur, M. J., Cecere, A., Wolf, S., et al. (2024). Global influence of soil texture on ecosystem water limitation. *Nature*, 635(8039), 631–638. https://doi.org/10.1038/s41586-024-08089-2
- Wu, R., & Kinter, J. L., III. (2009). Analysis of the relationship of U.S. droughts with SST and soil moisture: Distinguishing the time scale of droughts. *Journal of Climate*, 22(17), 4520–4538. https://doi.org/10.1175/2009JCL12841.1
- Yan, H., Xie, Z., Jia, B., Qin, P., Xia, Z., Dai, Q., et al. (2024). Estimation of soil moisture thresholds for aggravation of global terrestrial carbon uptake losses. *Journal of Geophysical Research: Atmospheres*, 129(5), e2023JD040392. https://doi.org/10.1029/2023jd040392
- Yang, L., Sun, G., Zhi, L., & Zhao, J. (2018). Negative soil moisture-precipitation feedback in dry and wet regions. Scientific Reports, 8(1), 4026. https://doi.org/10.1038/s41598-018-22394-7
- Yao, Y., Liu, Y., Zhou, S., Song, J., & Fu, B. (2023). Soil moisture determines the recovery time of ecosystems from drought. Global Change Biology, 29(13), 3562–3574. https://doi.org/10.1111/gcb.16620
- Yin, J. B., Gentine, P., Slater, L., Gu, L., Pokhrel, Y., Hanasaki, N., et al. (2023). Future socio-ecosystem productivity threatened by compound drought-heatwave events. *Nature Sustainability*, 6(3), 259–272. https://doi.org/10.1038/s41893-022-01024-1
- Yuan, X., Wang, Y., Ji, P., Wu, P., Sheffield, J., & Otkin, J. A. (2023). A global transition to flash droughts under climate change. *Science*, 380(6641), 6–191. https://doi.org/10.1126/science.abn6301
- Zeng, D., Yuan, X., & Roundy, J. K. (2019). Effect of teleconnected land-atmosphere coupling on northeast China persistent drought in spring-summer of 2017. *Journal of Climate*, 32(21), 7403–7420. https://doi.org/10.1175/JCLI-D-19-0175.1
- Zhang, J., Wang, S., Huang, J., He, Y., & Ren, Y. (2023). The precipitation-recycling process enhanced extreme precipitation in Xinjiang, China. Geophysical Research Letters, 50(15), e2023GL104324. https://doi.org/10.1029/2023GL104324
- Zhao, T., & Dai, A. (2022). CMIP6 model-projected hydroclimatic and drought changes and their causes in the twenty-first century. *Journal of Climate*, 35(3), 897–921. https://doi.org/10.1175/JCLI-D-21-0442.1
- Zhou, S., Williams, A. P., Lintner, B., Berg, A. M., Gentine, P., Keenan, T. F., et al. (2021). Soil moisture–atmosphere feedbacks mitigate declining water availability in drylands. *Nature Climate Change*, 11(1), 38–44. https://doi.org/10.1038/s41558-020-00945-z
- Zhou, S., Williams, A. P., Lintner, B. R., Findell, K. L., Keenan, T. F., Zhang, Y., & Gentine, P. (2022). Diminishing seasonality of subtropical water availability in a warmer world dominated by soil moisture–atmosphere feedbacks. *Nature Communications*, 13(1), 5756. https://doi.org/10.1038/s41467-022-33473-9
- Zomer, R. J., Xu, J., & Trabucco, A. (2022). Version 3 of the global aridity index and potential evapotranspiration database. *Scientific Data*, 9(1), 409. https://doi.org/10.1038/s41597-022-01493-1

HU ET AL. 10 of 10